Pickering emulsions stabilized by biodegradable dextran-based nanoparticles featuring enzyme responsiveness and coencapsulation of actives

Valentin Maingret, Coraline Chartier, Jean-Luc Six, Véronique Schmitt, Valérie Héroguez

Pickering emulsions stabilized by biodegradable dextran-based nanoparticles featuring enzyme responsiveness and co-encapsulation of actives

Valentin Maingret [a,b], Coraline Chartier [a,b], Jean-Luc Six [c], Véronique Schmitt [a,*], Valérie Héroguez [b,*]

[a] Centre de Recherche Paul Pascal, Univ. Bordeaux, CNRS, UMR 5031, 115 avenue du Dr Albert Schweitzer, 33600 Pessac, France.

[b] Laboratoire de Chimie des Polymères Organiques, Univ. Bordeaux, CNRS, Bordeaux INP, LCPO, UMR 5629, F-33607 Pessac, France.

[c] Université de Lorraine, CNRS, LCPM, F-54000 Nancy, France.

*corresponding authors
veronique.schmitt@crpp.cnrs.fr
heroguez@enscbp.fr

Abstract

In this study, Pickering emulsions of dodecane and medium chain triglyceride (MCT) oils were stabilized by simply alkylated-dextran nanoparticles. Our findings show that very little of these bio-friendly nanoparticles is necessary to stabilize Pickering emulsions while providing a high time stability (more than a year at 37°C). As dextran is known to be cleavable by dextranase enzyme, hydrolysis of the nanoparticles in the presence of dextranase could be achieved. This allowed performing on-demand destabilization of Pickering emulsions. Furthermore, two different fluorescent probes were loaded into the stabilizing particles and the oil droplets respectively, providing a proof of concept for co-encapsulation of actives in advanced delivery applications. Additionally, to a conventional fluorescence probe, quinine, an antimalarial drug was also encapsulated into the nanoparticles.

Keywords: Biodegradation, stimuli-responsiveness, encapsulation, sustainable release, dextranase, fluorescence.

1. Introduction

Pickering emulsions appear as a sustainable alternative to conventionally surfactant-stabilized emulsions (Arditty et al., 2004; Binks, 2002; Pickering, 1907; Ramsden, 1903). As they possess a much higher time stability, conferring them stimuli-responsiveness have enabled the design of robust on-demand release vectors (Dupont et al., 2021; Harman et al., 2019; Tang et al., 2015). In general, this stimuli-responsiveness comes from the ability of the stabilizing particles to desorb from the interface when subjected to a stimulus. On the threshold of their implementation in products at the industrial scale, some issues may be raised such as life cycle analysis. In most cases, such nanoparticles are exclusively made of synthetic materials or possess poor (bio)degradability at medium time scale (<year) meaning that they could accumulate once desorbed. The use of bio-sourced and/or (bio)degradable particles for the stabilization of stimuli-responsive Pickering emulsions is thus at stake for numerous applications including drug-delivery, cosmetics, agriculture or life sciences (Glasing et al., 2018; Liu et al., 2012; Qi et al., 2018). In this respect, we recently promoted the use of a natural polysaccharide, dextran, as a new brick material for the design of stabilizing nanoparticles with stimuli-responsiveness to pH and light, provoking their degradation into solutes (Maingret et al., 2020, 2021). Dextran is produced from bacteria like *leuconostoc mesenteroides* and its saccharide bonds can be split by dextranase (dextran-1,6-glucosidase), an enzyme which is expressed by many living organisms, including human beings (in spleen, liver, lungs) (Baldwin & Kiick, 2010). Various studies focused on the use of this natural polymer to design new nanostructures for biomedical applications for instance (Abid et al., 2020; Aumelas et al., 2007; Banerjee & Bandopadhyay, 2016; Celik et al., 2019; El Founi et al., 2018; Ren et al., 2018; Vercauteren et al., 1992). Specifically, as dextran is hydrophilic, hydrophobic modifications were performed to enable self-assembly of modified chains into nanoparticles. In this work, we propose an original strategy to produce highly stable Pickering emulsions stabilized by enzyme-

sensitive biodegradable dextran-based nanoparticles. First, we chose to use a simple modification step involving the grafting of alkyl chains onto dextran (Alkyl-dextran) and to produce nanoparticles from these (Aumelas et al., 2007; Kulthida Kaewprapan et al., 2012). Then, for the first time we stabilized Pickering emulsions using tiny amounts of such nanoparticles: as low as 0.02%wt of the total emulsion weight. That was made possible thanks to the small required coverage of the stabilized droplets and the low density of the nanoparticles, which was demonstrated by Multi Angle Light Scattering (MALS) measurements. Owing to the low overall modification of dextran chains which constituted the nanoparticles, alkyl-dextran chains could be still lysed by dextranase enzyme (Kulthida Kaewprapan et al., 2012). This was assessed by studying the hydrolysis of alkyl-dextran nanoparticles in presence of dextranase in a controlled pH medium, which took two days. We also observed controlled destabilization of Pickering emulsions of dodecane or biocompatible Medium Chain Triglyceride (MCT) oils in the same conditions with slower kinetics (month scale). Furthermore, study of multi-encapsulation sites in simple Pickering emulsions or derived capsules (actives located in dispersed phase and in stabilizing particles)has been addressed only to a limited extent but has been ongoing (Beladjine, 2019; Chen et al., 2020; Sakellari et al., 2021; Schröder et al., 2020). The second encapsulation site (stabilizing agents) allows confining a substance which activity is enhanced at the interface (like antioxidants). So, as an additional functionality, we propose in this work a proof of concept for the encapsulation of fluorescent probes inside the stabilizing particles and the oil droplets, which could be well visualized in confocal fluorescence microscopy. As an applicative step forward, quinine, an antimalarial drug was also encapsulated in the nanoparticles. Finally, as this biofriendly system features the possibility to trigger a single or double delivery of actives in presence of enzymes, it may find interest in many applicative fields like bio-catalysis, phytosanitary engineering or cosmetics.

2. Experimental section

2.1. Materials

Dextran (Mw = 34,000 g/mol, Mn = 26,000 g/mol, Đ= 1.3 as measured by the authors using Size-Exclusion Chromatography (SEC)) and dodecane (99%) were purchased from ABCR. 1,2-epoxyoctane (99%) was purchased from Alfa Aesar. Medium-chain triglyceride (MCT) "Miglyol 812N" was graciously provided by Stéarinerie Dubois. Hydrated tetrabutylammonium hydroxide (hydrated TBAOH), dextranase from *Penicillium sp*. lyophilized powder (100-250 units/mg protein) and BODIPY fluorescent probe (Fluorescein isothiocyanate channel, λ_{ex}=493; λ_{em}=503) (BDP_{FITC}) were purchased from Sigma Aldrich. A second BODIPY fluorescent probe (Texas Red channel, λ_{ex}=589; λ_{em}=616) (BDP_{TR}) was purchased from Lumiprobe. Quinine (99%) was purchased from Acros. All solvents used were of analytical grade.

2.2. Equipment and methods

Synthesis products characterization by proton Nuclear Magnetic Resonance (^{1}H NMR) was performed on a Bruker Advance 400 MHz apparatus. Nanoparticle size characterization was done with a NanoZS90 Dynamic light scattering (DLS) instrument (Malvern Instrument Ltd., UK) at a scattering angle of 90°. Multi Angle Light Scattering (MALS) experiments were performed on an ALV-5000 goniometer equipment where static scattering measurements were done every 5° from 50° to 150°. From the collected data, the average hydrodynamic diameter z and Polydispersity index (PDI) were determined. PDI is linked to z and its standard deviation σ as follows (eq.1):

$$PDI = \left(\frac{\sigma}{z}\right)^2 \quad (1)$$

Nanoparticles were also characterised by Transmission Electron Microscopy (TEM) on a HITACHI H-600 instrument (HV = 75 kV). Pickering emulsions were visualized by optical microscopy on a Zeiss Axioskop 40 apparatus in bright field and picture acquisition were done with a digital camera linked to the microscope. ImageJ software allowed measuring the size of around 200 droplets from these pictures. The data were then used to compute the average Sauter diameter (D[3,2], eq.2)):

$$D[3,2] = \frac{\sum_i^n d_i^3}{\sum_i^n d_i^2} \quad (2)$$

where d_i is the diameter of a drop from a n-drops population. The Sauter diameter is defined as the surface-average diameter of the drops. A typical standard deviation σ_d was also calculated to describe the drop size distribution width of the emulsions. For the encapsulation of fluorescence probes inside the nanoparticles, Fluorescence Spectroscopy (Jasco FP-8500 Fluorescence Spectrometer) was used to quantify the encapsulation efficiency and the loading capacity. Confocal fluorescence microscopy was used to visualize Pickering emulsions with two different encapsulated (in the nanoparticles and in the oil droplets) fluorescent probes.

2.3. Synthesis of alkylated dextran

The modification of dextran with alkyl moieties was adapted from the work of Rouzes *et al.*(Rouzes et al., 2003). Typically, 10 g (62 mmol of glucosidic units) of dextran were dissolved in 100 mL of DMSO at room temperature. After complete dissolution, 40 g (corresponding to 16.25 mmol of pure TBAOH, 0.27 eq.) of hydrated TBAOH were introduced along with 7.69 g (60 mmol, 0.97 eq.) of 1,2-epoxyoctane. After 48h of reaction at room temperature, the crude product was precipitated in EtOH and dialyzed 10 times against a H_2O/EtOH 50/50 v/v solution and then against pure water. The purified product was finally lyophilized and analysed using ^{1}H NMR as well as initial reagents (**Fig. S1-S3**). The yield of

the reaction is about 79%. Substitution of hydroxyl moieties (τ_{alkyl}) was then calculated by direct comparison of peaks area from protons of dextran and of grafted alkyl chains. Dextran mass composition (Φ^{m}_{Dex}) of alkyl-dextran chains was deduced from the latter (eq. S1-S2).

2.4. Nanoprecipitation of alkylated dextran

Nanoparticles of alkylated dextran were obtained through the nanoprecipitation process. To do so, alkyl-dextran chains (100 mg) were first solubilized into a solution of THF/H_2O 90/10 v/v (20 mL) and loaded into a syringe. Using a Chemyx Fusion 101 Syringe Pump, the polymer solution was added at a rate of 0.4 mL/min in a water bath (40 mL) which is a non-solvent of the alkyl-dextran chains. The dispersion was then purified by evaporating THF with a rotary evaporator, then three dialyses against pure water were performed and lasted 6 h, 12 h and 24 h. Finally, the purified aqueous dispersion of nanoparticles was concentrated by partly evaporating water. Dry residual weight technique was then used to calculate the concentration of nanoparticles into the dispersion. Typically, the yield of the nanoprecipitation step after purification is of 70%. Several dispersions of nanoparticles were produced and used throughout this work, they will be called NPDx in the following where x relates to the dispersion batch number.

The swelling of the nanoparticles was quantified by comparison of the density of free alkylated dextran chains at dry state (1.37, determined by pycnometry) to the average polymer density in the nanoparticle (determined by MALS). The proportion of absorbed water, $\%m_{water}$, is expressed as the ratio between the nanoparticle dry mass (m_D) and the mass of water contained in a swollen nanoparticle (m_w) as follows (eq. 3) (Pang et al., 2011):

$$\%m_{water} = \frac{m_w}{m_D} \quad (3)$$

Hypothesizing ideal mixing and considering that the mass of a dry nanoparticle is equal to the mass of the polymer it contains, the previous relation can be then written as (eq. 4):

$$\%m_{water} = \frac{(V_S - V_D) * \rho_{water}}{V_S * \rho} \quad (4)$$

where V_S and V_D are the volumes of the nanoparticle in its swollen and dry state respectively and ρ is the average polymer density in the swollen nanoparticle as mass preservation gives $m_D = m_{polym} = V_S * \rho$. The geometrical radius of the swollen nanoparticle obtained from MALS measurements (median value between R_h and R_g) was chosen to calculate V_S. The water mass fraction content Φ_w^m of a swollen nanoparticle can be finally expressed as follows (eq. 5):

$$\Phi_w^m = \frac{\%m_{water}}{1 + \%m_{water}} \quad (5)$$

2.5. Formulation of Pickering emulsions

Pickering emulsions were formulated with dodecane (or MCT oil) and with diluted alkyl-dextran nanoparticle aqueous dispersion. The shearing source was an Ultra Turrax (IKA T25) with a shaft (S25N 10G) used at a speed of 20,000 rpm for 2 min. As a first attempt, emulsion composed of 50/50 water/oil was formulated to determine the emulsion type. More precisely, aliquots of the produced emulsion were withdrawn and introduced in water and oil media respectively. As the aliquots dispersed well in water and not in oil, formation of an O/W emulsion was confirmed. In the following of this work, only O/W Pickering emulsions were formulated. The water/oil phase ratio used was always set to 80/20 v/v and the emulsion total volume was equal to 10 mL.

2.6. Enzymatically induced destabilization of Pickering emulsions

Destabilization of Pickering emulsions was studied in two steps. First, nanoparticle degradation in presence of dextranase was assessed and required conditions were determined. Then, the same conditions were adapted for Pickering emulsions.

2.6.1 Biodegradation of nanoparticles

Enzymatic degradation of dextran by dextranase was done in a 5 mM buffer aqueous medium. More specifically, a pH 5.6 McIlvain buffer was prepared by mixing a solution of citric acid (42 mM) with a solution of disodium phosphate dihydrate (116 mM) (Crepon et al., 1991). To study the degradation of alkyl-dextran nanoparticles by dextranase, three different dispersions of nanoparticles (0.5 mg/mL) were prepared. The first one was left aside as a control sample. In the second one, dextranase was added along with pH 5.6 McIlvain buffer so that their concentrations were equal to 0.05 mg/mL and 5 mM respectively in the dispersion. In the third dispersion, only McIlvain buffer was added to reach the same concentration (5 mM). The three dispersions were then placed on a stirring plate at 50 rpm inside a thermostatic incubator at 37°C. DLS measurements were performed on small aliquots at several time intervals to look for size changes.

2.6.2 Pickering emulsion destabilization

In this study, dodecane and MCT oil were used separately to formulate two series of four identical Pickering emulsions of 10 mL (*i.e.* 8 emulsions in total) with a concentration of nanoparticles (from NPD3) of 0.6 mg/mL of oil. For the formulation with MCT oil series, NaCl salt (10 mM) was added prior to emulsification as it provided better stability. Then, for each emulsion, 2 mL of different solutions were added (graphical description is available in **Fig. S4**) to screen different destabilisation conditions. In the two first emulsions of the two series (dodecane and MCT oil), 2 mL of a solution of McIlvain buffer was added so that its

concentration reached 5 mM in the continuous phase. In the second one, 2 mL of a dextranase solution (corresponding to 0.12 mg of enzyme) were added. In the third one, 2 mL of a solution of both McIlvain buffer and dextranase (same concentrations as before) were added. Finally, in the fourth one, 2 mL of pure water were added as control samples. The eight emulsions were then placed on stirring plate at 50 rpm inside a thermostatic incubator at 37°C. Macroscopic observations and pictures were done at several time intervals.

2.7. Double encapsulation of fluorescent actives

An active, either BDP_{TR} or quinine was encapsulated inside the nanoparticles. A second one, BDP_{FITC}, was encapsulated into the oil droplets of Pickering emulsions.

2.7.1. Encapsulation of actives inside the nanoparticles

The nanoprecipitation procedure was adapted for the encapsulation inside the nanoparticles. BDP_{TR} fluorescent probe encapsulation was done by solubilising 0.1%wt of the probe (relative to the polymer concentration) in the alkylated dextran solution. In the case of quinine, 50%wt of probe (relative to the polymer concentration) were introduced. Then injection was done according to a 1/10 v/v [solvent (THF/H_2O 90/10 v/v)]/[non-solvent (H_2O)] ratio to foster precipitation of the polymer and the active at similar speeds (Trofymchuk et al., 2019). Finally, dialysis of the obtained dispersions (100 mL) were done against 5 L of pure water, three times for 6 h, 12 h and 24 h. In the following, dispersions of loaded alkyl-dextran nanoparticles will be called NPD-BDP_{TR} and NPD-Quinine. To evidence the encapsulation of BDP_{TR}, DLS and fluorescence spectroscopy were used. First, size distribution analysis and Derived Count Rate (DCR) measurements were performed to quantify the relative amount of nanoparticles. As a reminder, DCR value is directly related to the concentration of nanoparticles

and their size. Then, the nanoparticle dispersion was centrifugated at 13,000 rpm during 25 min which resulted in the formation of a pellet (rich in nanoparticles) and a supernatant (in which the nanoparticle concentration is low). The pellet was re-dispersed in a minimum amount of solvent so that two dispersions of nanoparticle with different concentrations were obtained. The same measurements as before (size and DCR) were then performed on the supernatant and the re-dispersed pellet. Residual dry weight technique allowed to determine polymer concentration at each step (before centrifugation, in the supernatant, in the re-dispersed pellet). Finally, fluorescence intensity values at an excitation wavelength of 590 nm of the different nanoparticle dispersion fractions were measured at 620 nm. Then, to quantitatively appreciate the encapsulation of both actives, loading capacity and encapsulation efficiency were computed as follows (Abid et al., 2020)(eq.6-7):

$$encapsulation\ efficiency = \frac{wt.of\ entrapped\ drug}{wt.of\ total\ drug} * 100 \quad (6)$$

$$loading\ capacity = \frac{wt.of\ entrapped\ drug}{wt.of\ nanoparticle} * 100 \quad (7)$$

The quantity of entrapped drug was determined by fluorescence spectroscopy. First, calibration curves (**Fig. S5**) of BDP_{TR} and quinine were done using THF/H_2O 90/10 v/v as solvent. For BDP_{TR} (and quinine respectively), concentrations ranged from 0.005 μg/mL to 0.1 μg/mL (from 0.075 μg/mL to 0.75 μg/mL respectively), excitation wavelength was 590 nm (350 nm respectively) and emission was recorded between 600 and 695 nm with a maximum emission at 621 nm (between 370 and 590 with a maximum emission at 445 nm respectively). Nanoparticle dispersions (at a known concentration) were lyophilized and solubilized in a THF/H_2O 90/10 v/v solution and the fluorescence intensities of the mixes were measured. By

knowing the initial concentration of the dispersions (residual dry weight), it was finally possible to compare it to the concentration of drug measured *via* fluorescence spectroscopy.

2.7.2. Pickering emulsion with double encapsulation of fluorescence probes

Encapsulation inside the droplets was done by solubilizing BDP_{FITC} probe in dodecane (0.0002 wt%) prior to emulsification step. The latter was obtained with an Ultra Turrax at 15 krpm during 45s and loaded BDP_{TR} nanoparticles concentration was 0.8 g/L of oil. The presence of fluorescent dyes did neither influence the emulsification nor the stability. The emulsions were then observed with a confocal fluorescence microscope. Excitation wavelength of BDP_{TR} (inside the stabilizing nanoparticles) was set to 560 nm instead of 590 nm likely due to solvatochromic effect. To better discriminate the two different probes, the green channel (corresponding to the fluorescence emission of BDP_{FITC}) was switched in blue *via* the microscope software. Pictures of a specific area were taken at different z-depths (around 6 μm wide from bottom to top). Z-stacks of these pictures were then treated *via* ImageJ and an interactive 3D view of the re-constructed droplets with the two fluorescence channels was produced.

3. Results and discussion

3.1. Synthesis of alkylated dextran

Dextran was modified through etherification with 1,2-epoxyoctane using hydrated TBAOH (**Fig. 1**). According to ^{1}H NMR results, substitution of hydroxyl moieties could be determined and was equal to 66% (maximum is 300% as glucosidic units hold three hydroxyl units) (**Fig. S1-S3**, eq. S1). In other words, Alkyl-dextran chains were made of 65%wt of

dextran and of 35%wt of alkyl chains, witnessing that dextran was only slightly modified (eq. S2).

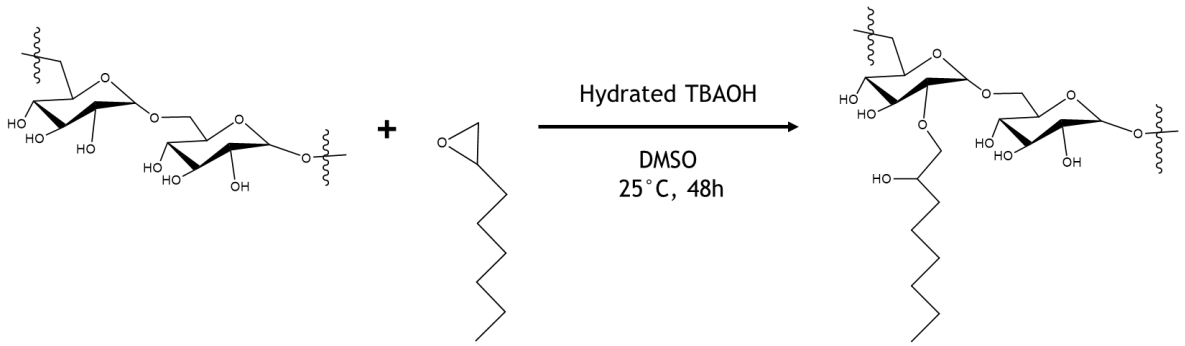

Fig. 1. Reaction scheme for the formation of Alkyl-dextran from dextran and 1,2-epoxyoctane.

3.2. Nanoprecipitation of alkylated dextran

Nanoprecipitation of Alkyl-dextran into water produced well defined spherical nanoparticles with a narrow monomodal size distribution as shown by TEM (**Fig. 2**) and DLS data (**Table 1**). As a result, four different nanoparticle dispersions were obtained and were pretty the same in terms of size distribution range. In the following, the used dispersion will be specified. After characterization, nanoparticle dispersions were stored hidden from the light in a cupboard. They could be stored for more than 4 months without major stability issues (**Fig. S6**).

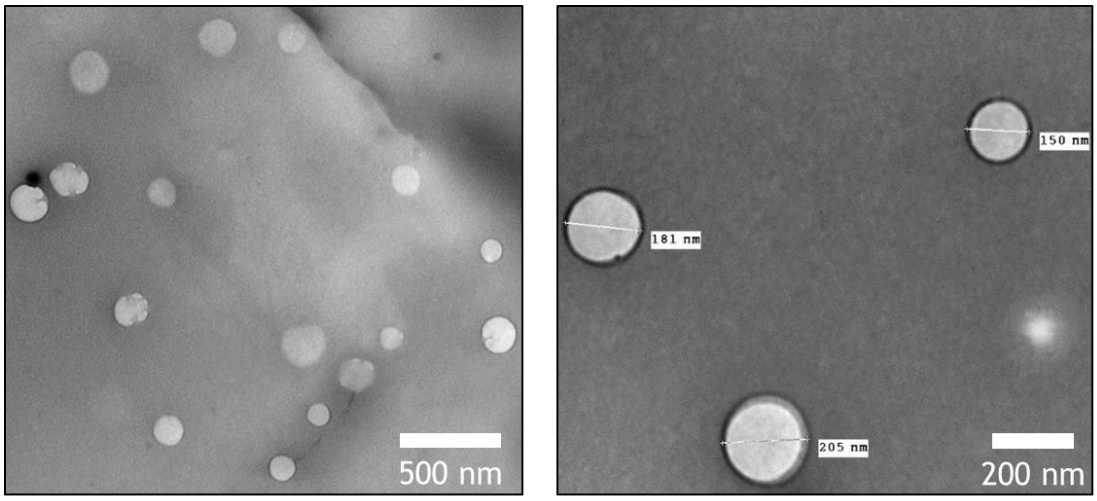

Fig. 2. TEM pictures of alkyl-dextran nanoparticles from NPD1.

Nanoparticles on TEM pictures presented a contrasted small shell (from grey to black), which may indicate a core-shell or vesicle like morphology. From these pictures, a D[4,3] of 175 ± 32 nm (n = 19, the statistics is low due to a limited number of TEM micrographs) was calculated. This value is bigger than the one obtained from DLS measurements, which may come from the spreading of the nanoparticles under vacuum when using TEM.

Table 1. Size distributions of alkyl-dextran nanoparticle dispersions (without active)

Nanoparticle dispersion batch	NPD1	NPD2	NPD3	NPD4
Average hydrodynamic diameter (DLS 90°)	125 ± 42 nm	153 ± 59 nm	150 ± 49 nm	149 ± 54 nm
Polydispersity index (PDI)	0.114	0.147	0.105	0.130

To investigate more in depth their properties, MALS measurements were done on nanoparticles from NPD4 (**Fig. S7-S10,** eq. S3-S10). Static Light Scattering results were analysed with a Guinier plot, which allowed to determine the molar mass (M_w) and the radius of gyration (R_g) of the objects. Furthermore, it was then possible to calculate the average

polymer density inside the nanoparticles, which is a requirement for the calculus of droplet coverage in the formulation section (**Table 2**).

Table 2. MALS results obtained with nanoparticles from NPD4

Molar mass (M_w)	Radius of gyration (R_g)	Geometrical radius (a_m)	Average structural polymer density (ρ)
9.321 10^7 g/mol (± 1.6 %)	62.9 nm (± 7.5 %)	58.6 nm (± 7.5 %)	0.183 g/cm^3 (± 20 %)

The average structural polymer density is extremely low, meaning that most of the nanoparticle is constituted of water. More precisely, the proportion of water absorbed (eq. 4) was equal to 4.73 involving that the water mass fraction Φ_w^m (eq. 5) inside the nanoparticles was then equal to 83%. That means the nanoparticles are in average composed of 83wt% of water and 17wt% of the alkylated dextran. Hydrodynamic radius was also computed from multi angle DLS and was found equal to 69.7 nm (**Fig. S7**), corresponding to a diameter of 139.6 nm, in good agreement with the value reported in **Table 1** and which should be more accurate than DLS at 90°. R_g/R_h was equal to 0.90 (close to 1, a value corresponding to vesicles) which may indicate an aqueous core / alkylated dextran shell organization, in agreement with TEM pictures (**Fig. 2**). However, small angle neutron scattering (SANS) would be required to further describe the morphology of these nanoparticles.

3.3. Formulation of O/W Pickering emulsions

3.3.1. Determination of emulsion type

Pickering emulsions with a water phase/oil phase ratio equal to 50/50 v/v were first formulated to assess the type of emulsion. Only O/W emulsions were formed. All the Pickering emulsions formulated in this work macroscopically creamed quite quickly because of the low density of dodecane (0.75 g.cm^{-3}) compared to water and the large size of the droplets.

3.3.2. Droplet size relationship with nanoparticle concentration – limited coalescence phenomenon

One of the most interesting feature of Pickering emulsion is the limited coalescence phenomenon. After shearing the water and oil phases, large amounts of interface are created. When this quantity of interface is higher than the one which can be stabilized by the introduced nanoparticles, coalescence occurs leading to a decrease of the interfacial area. As nanoparticles are irreversibly adsorbed to the interface, coalescence between droplets increase their coverage. Coalescence events continue until droplets are enough covered and remain stable. At that point, the Sauter diameter of the droplets can be related to the quantity of introduced nanoparticles as shown in eq. 8 (~~S~~Arditty et al., 2003; Schmitt et al., 2014):

$$\frac{1}{D[3,2]} = \frac{c}{4C\rho d_p} \quad (8)$$

where c is the concentration of polymer constituting the nanoparticles relative to the volume of the dispersed phase (computed with the residual dry weight technique), ρ is the average polymer density in the nanoparticle (calculated in the previous section and equal to 0.183 g/cm^3), C is the surface coverage, that is, the fraction of the droplet interfacial area covered by particles, and d_p is the stabilizing particle diameter (assimilated to the geometrical diameter provided by the MALS experiments see **Table 2**). In general, particles are not swollen, and their absolute density is known. In our case, we used the residual dry weight to compute the amount of stabilizing material constituting the nanoparticles and the average structural density of polymer inside them to similarly recover a quantity of stabilizing entities. It has been shown in previous studies that

the limited coalescence phenomenon allows obtaining narrow monomodal size distributions of droplets in a repeatable way (~~S~~-Arditty et al., 2003; Whitesides & Ross, 1995). The linear relationship between the inverse of the Sauter diameter and the concentration of nanoparticles is valid in the low concentration range. For larger particle concentrations, as there are enough particles to stabilize the created interface, the drops size distribution generated by the process is frozen. The size of the droplets is then dictated by the process and becomes independent of the nanoparticle concentration, that is, a plateau is reached. Our results obtained by varying the amount of nanoparticles are in accordance with the limited coalescence phenomenon as we clearly observed a linear relationship (in agreement with eq. 8) until around 1 mg/mL and then a plateau behaviour (**Fig. 3**). Detailed values of D[3,2] depending on the nanoparticle concentration are gathered in **Fig. S11**. Pickering emulsions stabilized by nanoparticles from another dispersion (NPD2) were also formulated and the limited coalescence curve was stacked to the one above, showing quite similar results despite the difference in diameter between NPD1 and NPD2 (**Fig. S12**) showing consistency. All these Pickering emulsions were stored in the same conditions as the stabilizing nanoparticles.

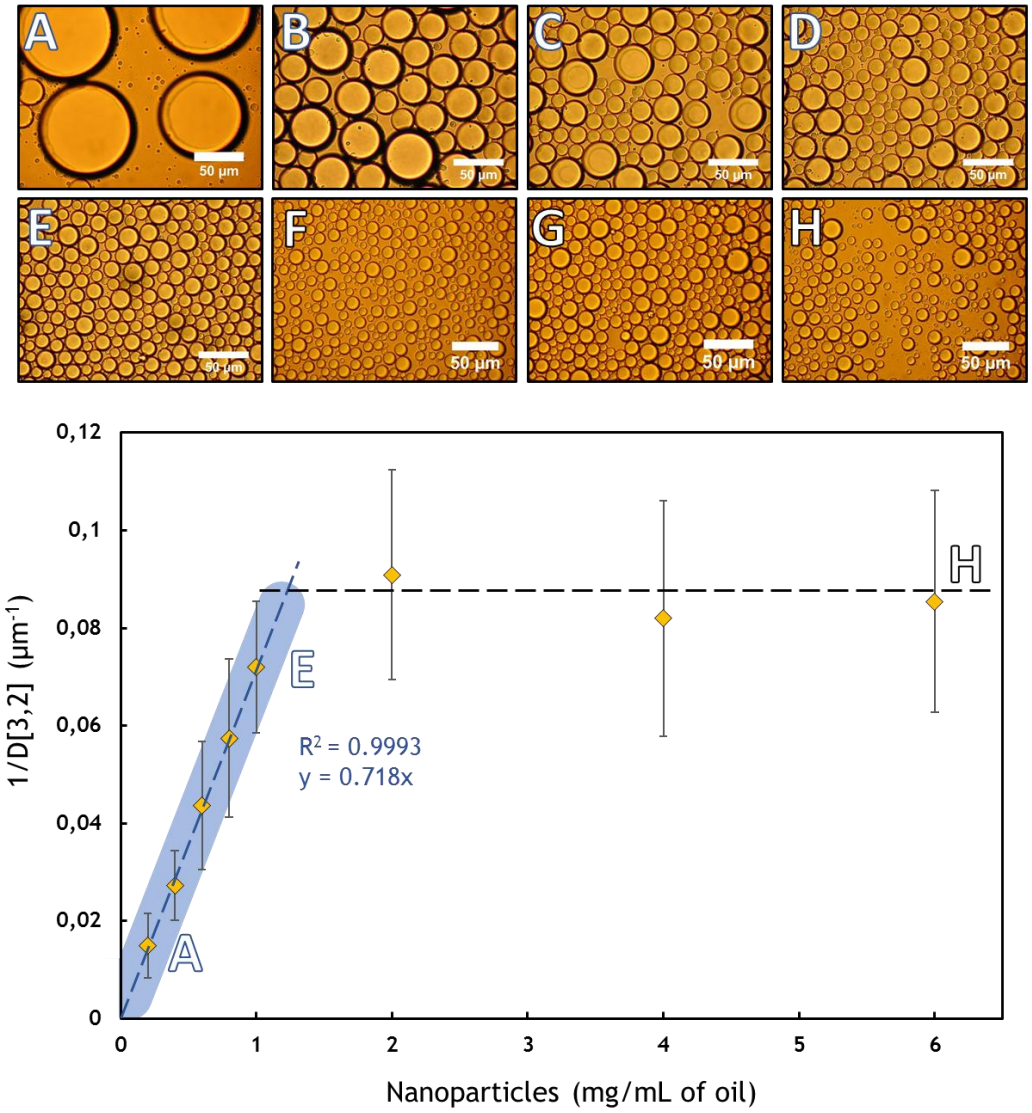

Fig. 3. Optical microscopy pictures of emulsions with various concentrations of nanoparticles (NPD1) from 0.2 (A) to 6 g/L (H) of oil, scale bar is equal to 50 μm (Top). Evolution of 1/D[3,2] as a linear function of the nanoparticle concentration at low values (limited coalescence domain in blue) followed by a plateau (black) (Bottom). All the emulsions were formulated following an oil/water ratio of 20/80 v/v.

From the limited coalescence relationship, the surface coverage of the droplets could be determined. Results from MALS experiments were used to obtain ρ and d values (ρ=0.183 mg/cm^3 and d=2*a_m=117.2 nm see **Table 2**). As a result, a surface coverage of 0.13 ± 0.04 was found for emulsions stabilised with NPD2 nanoparticles (**Fig. S12**, eq. S11). This value is dramatically low compared to a typical monolayer of hexagonally close-packed particles organization where C = 0.9 and compared to other Pickering emulsion systems in the literature

using PLGA nanoparticles (C=0.91) (Albert et al., 2018), cellulose nanocrystals (C=0.6 and above) (Kalashnikova et al., 2011), acetalized dextran nanoparticles (C=0.94) (Maingret et al., 2020), charged silica particles (C=0.54) (Ridel et al., 2016) and in other works (from 0.22 to 0.7) (Arditty et al., 2003; Nie et al., 2008). However, similar coverage or even lower were already observed in some previous studies. Gautier *et al*. work presented Pickering emulsions with a coverage of 0.08 from charged particles (Gautier et al., 2007) and Binks *et al*. approximated coverages below 0.2 using natural occurring spores (Binks et al., 2005). Vignati *et al*. obtained stable Pickering emulsions at a coverage value as low as 0.05 with charged particles (Vignati et al., 2003). The latter observed a diffusion of particles and concluded about the role of the particle dynamics in the stabilization of poorly covered drops. This behaviour has been later confirmed by Destribats *et al.* who clearly showed the accumulation of particles in the contact zones between drops (Destribats et al., 2014). In our case, nanoparticles are barely negatively charged (measured zeta potential around -20 mV in pure water).

Strikingly, this low coverage provides a high time stability since emulsions were still stable after 21 months of storage at room temperature (**Fig. S13**), and still after 1 year at 37°C also. They were not fragile as they could be easily handled without breaking. This system may then be of high interest for the sustainable design of Pickering emulsions as it requires very few amounts of stabilizing material.

3.4. Destabilization of Pickering emulsions

In a first set of experiments, enzymatic degradation of the nanoparticles was demonstrated. The corollary was then to show that the destabilization of these highly stable Pickering emulsions could be enzymatically induced. More precisely, destabilization of Pickering emulsions of dodecane which is a model oil in emulsion science was done first. Then, the same experiment

was done on Pickering emulsions using a biocompatible oil (medium chain triglyceride – MCT) as a further step towards applications in cosmetics or drug-delivery like.

3.4.1. Enzymatic degradation of the nanoparticles

Dextranase is an enzyme capable of lysing the α–(1,6) glucoside linkages between the glucosidic units constituting dextran chains. As a consequence of steric hindrance, it has been demonstrated that the higher the substitution of dextran, the lower its degradability (Crepon et al., 1991). Specifically, if the density of alkyl chains is too high, the biodegradation by dextranase enzyme is barely operating, or impossible. At a modification rate below 100% (compared to the theoretical possible 300%), the degradation has been shown to be working for small linear grafts (Aumelas et al., 2007; Kulthida Kaewprapan et al., 2012). However, it was not tested with Alkyl-dextran chains assembled into nanoparticles. It has also been shown that the enzymatic degradation of dextran by dextranase should be done in a slightly acidic pH-controlled medium with temperature control (Aumelas et al., 2007; Franssen et al., 1999; Kultida Kaewprapan et al., 2011). More specifically, former studies reported the use of a pH 5.6 McIlvain buffer and 37°C as incubation temperature (Crepon et al., 1991; Nouvel et al., 2009). Briefly as a reminder, three different nanoparticle dispersions with different conditions (injection of dextranase and McIlvain buffer, injection of McIlvain buffer, no injection (control)) were prepared and gently shaken at a controlled temperature of 37°C (Section 2.6.1). DLS and visual assessments were done to characterize the stability of the different dispersions as a function of time. In this study, buffer concentration was limited to 5 mM to avoid quick sedimentation of the slightly negatively charged NPs (measured zeta potential around -20 mV in pure water).

The size of the nanoparticles from the control sample did not change during 48 h and its macroscopic aspect remained bluish. In the sample where McIlvain buffer was added, the

measured size of the nanoparticles increased (700 nm after 24 h), making the dispersion more turbid. After 48 h, the dispersion remained turbid and the measured size was the same (around 800 nm) (**Fig. 4**). This is likely due to particle aggregation as a result of electrostatic screening by the electrolytes present in the buffer (Debye length estimated to 2.1 nm). In the dispersion, where both the McIlvain buffer and the dextranase enzyme were added, the dispersion became first turbid and the measured size increased from 200 nm to almost 600 nm in 4 h and then more than one micron after 24 h (**Fig. 4**). Size increase of the nanoparticles in presence of dextranase was already observed in previous works (PCL-grafted dextran nanoparticles with a size increase from 200 nm to 900 nm in 2 hours) (Villemson et al., 2006; Ydens et al., 2005) and was explained by the adsorption of dextranase onto the surface of nanoparticles and by the interactions between hydrophobic cores no longer protected by hydrophilic moieties of dextran. Therefore, ionic strength along with the addition of dextranase induced the increase of the measured size of the nanoparticles. However, after 24 h, the dispersion was already less turbid than at 4 h, indicating a decrease in the quantity of the nanoparticles (as the size increased during this interval). After 48 h, the dispersion was crystal clear, showing that nanoparticles were hydrolysed (**Fig. 4**). The size of the remaining nanoparticles is not totally reliable as the scattered signal in DLS was very low.

Although the concentration of the added buffer was limited to a low value of 5mM in this study to avoid sedimentation, degradation with dextranase was verified so that it could be implemented in Pickering emulsions.

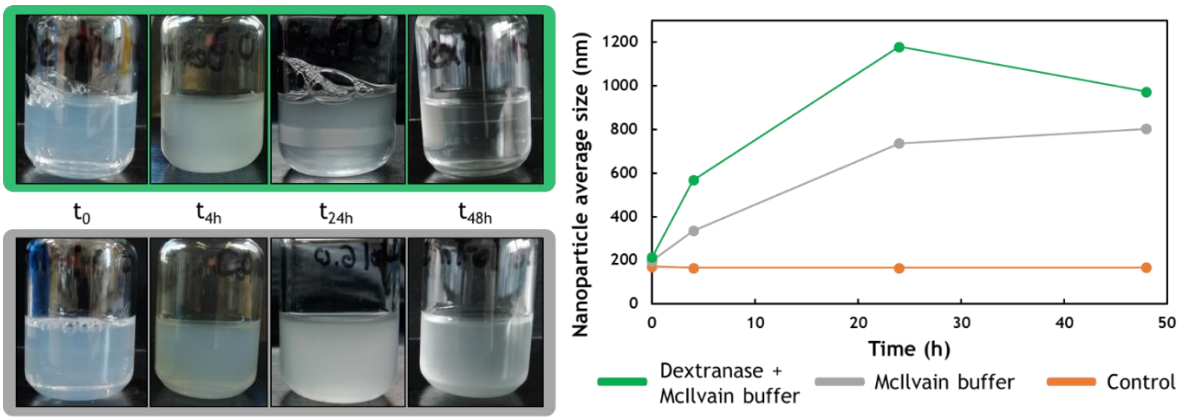

Fig. 4. Size and stability over time of several nanoparticle dispersions (form NPD3) under different conditions: with dextranase and McIlvain buffer (green), only with McIlvain buffer (grey), pure water control sample (orange). Pictures on the left show the macroscopic aspect of the dispersions at several times (green label is for dextranase and McIlvain buffer, grey is for McIlvain buffer only).

3.4.2. Pickering emulsion destabilization

Destabilization of Pickering emulsions of dodecane occurred only when both dextranase and McIlvain buffer were added in the continuous phase (**Fig. 5**). This destabilization was assessed macroscopically and appeared after 12 days when large oil droplets and a thin layer of oil could be observed. After 20 days, bigger and more numerous droplets could be observed as well as a thicker oil layer. Finally, after 60 days, as the layer of oil and that of the droplet randomly packed (occupying 64% of the volume) are of the same size, the volume of free oil is higher than the volume of emulsified oil, that is the destabilization can be relatively quantified as more than 50%. In the other conditions, no macroscopic destabilization was observed, and similar emulsions could be stored for more than a year at 37°C without stability issues.

Acidic pH did not lead to destabilization which confirm that even if nanoparticles are prone to destabilization with ionic strength, only dextranase make the destabilization of the emulsion occurring.

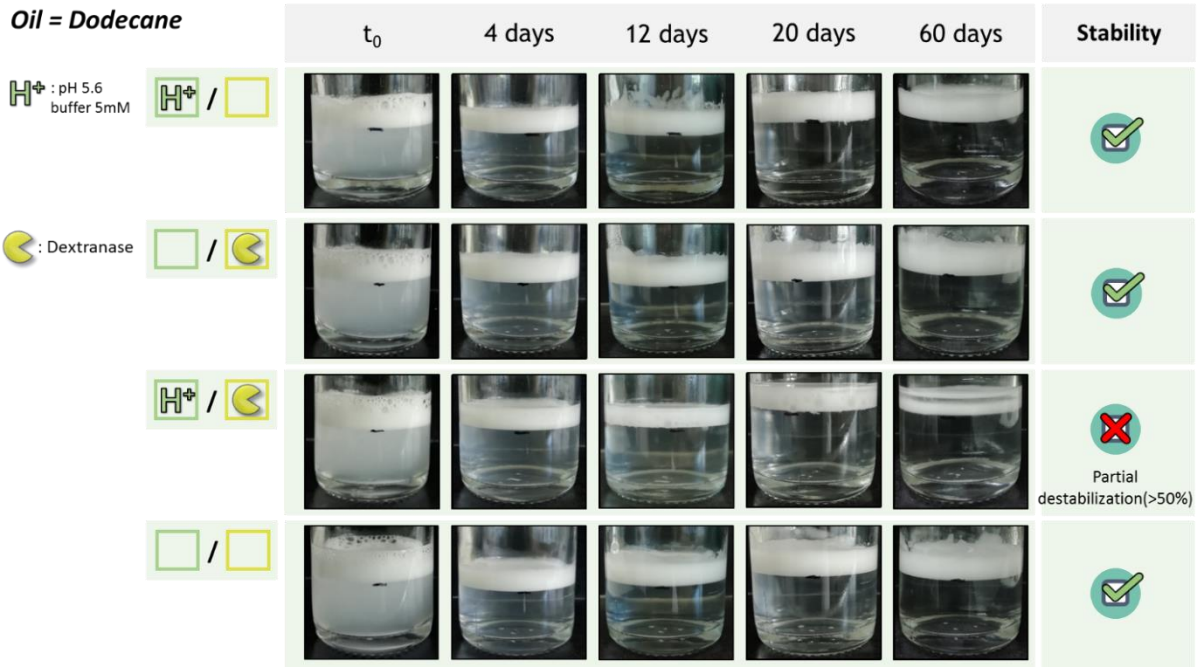

Fig. 5. Macroscopic aspects of dodecane emulsions over time – with only McIlvain buffer, with only dextranase, with McIlvain buffer and dextranase, control sample. Nanoparticles used to stabilize the emulsions came from NPD3. It should be noted that no stable emulsion can be obtained without particles.

Destabilization of Pickering emulsions is then delayed in time compared to the degradation of the nanoparticles. To modulate the destabilization time, several parameters could be changed. For instance, agitation of the rotary plate could be higher than 50 rpm, without inducing the destabilization of the emulsion. Moreover, McIlvain buffer concentration could be increased as it may not lead to irreversible destabilization compared to the study of nanoparticles in dispersion. Finally, dextranase concentration could be also increased to speed up the destabilization. Indeed, less surface of the nanoparticles is available for adsorption of dextranase and due to the weak agitation, more dextranase may be needed to reach similar kinetics as the previous study (48h). However, this slower kinetics can be seen as advantageous as it did not lead to a burst release, which is often problematic for some drug-delivery like applications (Liechty et al., 2010).

Surprisingly, using biocompatible MCT oil led to small changes in the macroscopic observations. Indeed, all emulsions were slightly or strongly flocculated, which may come from

the initial addition of 10 mM of salt (Debye length was then equal to 3 nm without McIlvain buffer or 1.75 nm with the buffer) (**Fig. S.14**). Moreover, the destabilization occurred also when dextranase was added alone, which was not expected. We do hypothesize that it could come from the nature of the oil which is more polar than dodecane and/or the addition of salt which may increase the enzyme activity.

3.5. Double encapsulation of fluorescent actives

Multi-encapsulation site systems are more and more studied and implemented in Pickering emulsion systems (Sakellari et al., 2021; Schröder et al., 2020). Herein, we encapsulated separately two different actives inside alkylated-dextran nanoparticles. As a proof of concept, a BDP_{TR} fluorescent probe was encapsulated. Alternatively, quinine, an antimalarial drug was encapsulated(Lavis & Raines, 2008). Loading capacity and encapsulation efficiency were determined using fluorescence spectroscopy. Another fluorescent probe, BDP_{FITC}, was encapsulated inside the oil droplets of a Pickering emulsion stabilized by BDP_{TR} loaded nanoparticles. Finally, confocal fluorescence microscopy allowed visualizing at different depths the two encapsulated probes.

3.5.1. Encapsulation of actives inside the nanoparticles

As described in the section 2.7.1., actives were encapsulated into the nanoparticles at the nanoprecipitation step by solubilizing the probe in the polymer solution to be injected. Encapsulation of BDP_{TR} inside the nanoparticles was demonstrated by DLS and fluorescence spectroscopy analyses of different fractions of a nanoparticle dispersion subjected to centrifugation. Results showed that the fluorescence intensity was directly related to the concentration of nanoparticles proving that encapsulation was achieved (**Fig. S15**). This

encapsulation was quantitatively characterized with calibrations curves done with THF/H_2O 90/10 v/v as solvent. Lyophilized loaded nanoparticles were hydrolysed in the same solvent and analysed (**Fig. S5** shows fluorescence spectroscopy measurements for BDP_{TR} encapsulation and **Fig. 6** for quinine encapsulation). Results obtained for both loaded nanoparticle dispersions are summarized in **Table 3**.

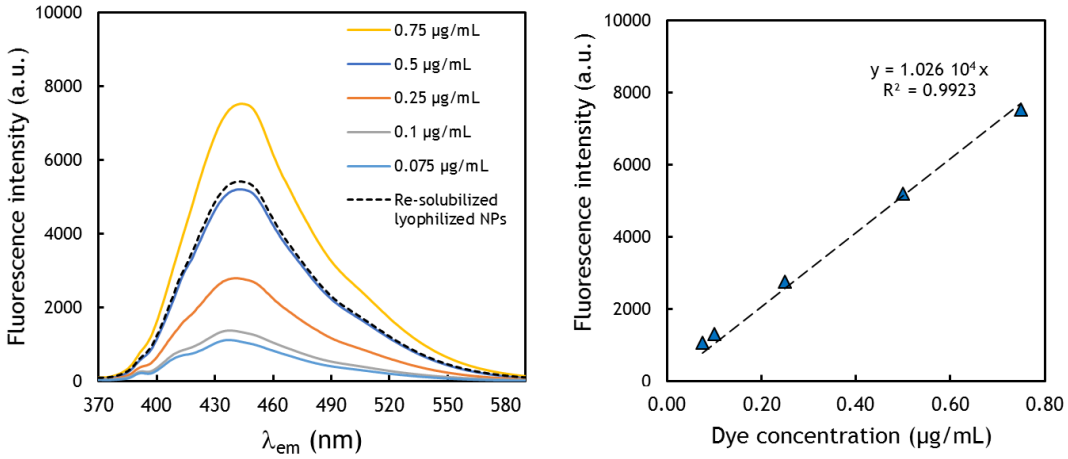

Fig. 6. Emission fluorescence spectroscopy spectra of quinine at different concentrations and of the re-solubilized lyophilized NPs from NPD-Quinine in THF/H_2O v/v 90/10 (λ_{exc} = 350 nm) (left), calibration curve using fluorescence emission intensities at 440 nm (right).

Table 3. Size, encapsulation efficiency and loading capacity of Alkyl-dextran nanoparticles loaded with BDP_{TR} or quinine actives

NPD-Active	Probe/Polymer initial ratio	Residual dry weight	Diameter (DLS 90°)	Loading capacity	Encapsulation efficiency
NPD-BDP_{TR}	0.1 wt%	0.4 mg/mL	143 ± 55 nm (PDI = 0.148)	0.00125 wt%	1.25 wt%
NPD-Quinine	50 wt%	0.35 mg/mL	115 ± 45 nm (PDI = 0.151)	0.15 wt%	0.3 wt%

Loading efficiency and loading capacity are very low (Kulthida Kaewprapan et al., 2012) for both probes but it may come from the extensive washing steps using dialysis (Abid et al., 2020). Nevertheless, for some specific applications, catalytic/therapeutic amounts of actives are required. Finally, small loadings do not change that much the overall composition of the

stabilizer and thus may not change the key properties of the nanoparticles which are their capacity to adsorb at interfaces and their biodegradability by dextranase. Despite this low encapsulation capacity, it was still possible to visualize nanoparticles around droplets of oil in confocal fluorescence microscopy as it is described in the following section. Higher values could be obtained by dismissing the dialysis step as done by Kaewprapan *et al*. for the encapsulation of lidocaine in modified-dextran nanoparticles (Kulthida Kaewprapan et al., 2012). However, the substitution degree of the dextran they used to obtain well dispersed loaded nanoparticles was much higher (150%) which is not suitable for biodegradation with dextranase. Still, optimization of both process and hydrophobicity while keeping biodegradation possible may improve our results which here stand mostly as a proof of concept.

3.5.2. Pickering emulsion with double encapsulation of fluorescence probes

Following the encapsulation of BDP_{TR} inside nanoparticles, formulation of Pickering emulsion using these stabilizers was performed. BDP_{FITC} probe was diluted into dodecane prior to emulsification. Stable Pickering emulsions were produced and were directly observed with a confocal fluorescence microscope. Using ImageJ, 3D view of z-stacked of pictures of a same area was built (**Fig. 7**).

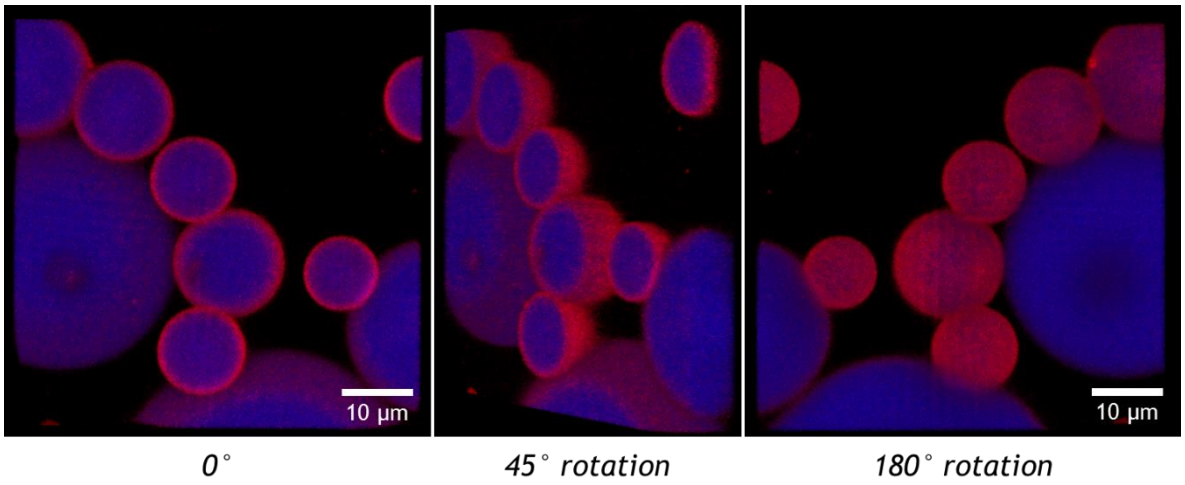

Fig. 7. 3D views of z-stacked pictures of Pickering emulsion droplets with multiple encapsulation sites obtained from confocal fluorescence microscopy (NPD-BDP_{TR}). BDP_{TR} encapsulated in the nanoparticles appear in red, BDP_{FITC} encapsulated in the emulsion droplets is coloured in blue.

Nanoparticles are well visible around droplets of blue coloured oil droplets. The coverage cannot be appreciated quantitatively but it can be noticed that it is incomplete as the inside of the droplets is visible on the 180° rotation of the 3D view. This proof of concept for the co-encapsulation of actives may be of interest for applications like dietary supplements or imaging in biological systems.

4. Conclusion

We showed that it is possible to formulate Pickering emulsions thanks to alkylated-dextran chains self-assembled into nanoparticles. Few amounts of this material are necessary to obtain a very long-time stability. Moreover, induced degradation of the nanoparticles and so destabilization of the formulated emulsions is rendered possible with addition of dextranase. As this enzyme can be found in many biological environments, the scope of applications of our system is widened. Finally, we were able to co-encapsulate two different fluorescent probes and visualise their loci *in situ*. An antimalarial drug, quinine could be also encapsulated into the nanoparticles, as a first step toward more applied delivery systems. As perspectives,

encapsulation into the nanoparticles can be further studied to increase encapsulation efficiency and loading capacity of the nanoparticles. Still, this system can be used as a common vector for lipophilic substances (large encapsulation capacity in the droplets) requiring very few amounts of biodegradable material and featuring long time stability for on-demand drug-delivery like applications.

Acknowledgments

V. Maingret acknowledges support from the Ministère de l'Enseignement Supérieur, de la Recherche et de l'Innovation for his Ph.D. grant. The authors thank their respective academic institution for financial support. The authors also acknowledge Emmanuel Ibarboure for his precious expertise in fluorescence and confocal microscopy experiments.

Supporting information

^{1}H NMR spectra of unmodified dextran, 1,2-epoxyoctane and alkylated-dextran, substitution degree of dextran calculus, Pickering emulsion destabilization set-up, emission fluorescence spectra of BDP_{TR} and calibration curve related, DLS analysis of NPD3 at t_0 and $t_{4months}$, MALS results of NPD4 (DLS and SLS), average structural polymer density of NPD4 nanoparticles calculations, detailed D[3,2] of droplets from limited coalescence curve, surface coverage calculation, stability of Pickering emulsions after 21 months, destabilisation study of biocompatible MCT oil Pickering emulsions, analyses of different BDP_{TR} loaded nanoparticles fractions isolated by centrifugation.

References

Abid, M., Naveed, M., Azeem, I., Faisal, A., Faizan Nazar, M., & Yameen, B. (2020). Colon

specific enzyme responsive oligoester crosslinked dextran nanoparticles for controlled release of 5-fluorouracil. *International Journal of Pharmaceutics*, *586*(June), 119605. https://doi.org/10.1016/j.ijpharm.2020.119605

Albert, C., Huang, N., Tsapis, N., Geiger, S., Rosilio, V., Mekhloufi, G., Chapron, D., Robin, B., Beladjine, M., Nicolas, V., Fattal, E., & Agnely, F. (2018). Bare and Sterically Stabilized PLGA Nanoparticles for the Stabilization of Pickering Emulsions. *Langmuir*, *34*(46), 13935–13945. https://doi.org/10.1021/acs.langmuir.8b02558

Arditty, S., Whitby, C. P., Binks, B. P., Schmitt, V., & Leal-Calderon, F. (2003). Some general features of limited coalescence in solid-stabilized emulsions. *Eur. Phys. J. E*, *11*(3), 273–281. https://doi.org/10.1140/epje/i2003-10018-6

Arditty, S, Whitby, C. P., Binks, B. P., Schmitt, V., & Leal-Calderon, F. (2003). Some general features of limited coalescence in solid-stabilized emulsions. *Eur. Phys. J. E*, *11*, 273–281. https://doi.org/10.1140/epje/i2003-10018-6

Arditty, Stéphane, Schmitt, V., Giermanska-Kahn, J., & Leal-Calderon, F. (2004). Materials based on solid-stabilized emulsions. *Journal of Colloid and Interface Science*, *275*(2), 659–664. https://doi.org/10.1016/j.jcis.2004.03.001

Aumelas, A., Serrero, A., Durand, A., Dellacherie, E., & Leonard, M. (2007). Nanoparticles of hydrophobically modified dextrans as potential drug carrier systems. *Colloids and Surfaces B: Biointerfaces*, *59*(1), 74–80. https://doi.org/10.1016/j.colsurfb.2007.04.021

Baldwin, A. D., & Kiick, K. L. (2010). Polysaccharide-modified synthetic polymeric biomaterials. *Biopolymers*, *94*(1), 128–140. https://doi.org/10.1002/bip.21334

Banerjee, A., & Bandopadhyay, R. (2016). Use of dextran nanoparticle: A paradigm shift in bacterial exopolysaccharide based biomedical applications. *International Journal of Biological Macromolecules*, *87*, 295–301. https://doi.org/10.1016/j.ijbiomac.2016.02.059

Binks, B. P. (2002). Particles as surfactants similarities and differences. *Current Opinion in Colloid & Interface Science*, *7*, 21–41.

Binks, B. P., Clint, J. H., Mackenzie, G., Simcock, C., & Whitby, C. P. (2005). Naturally Occurring Spore Particles at Planar Fluid Interfaces and in Emulsions. *Langmuir*, *21*(18), 8161–8167. https://doi.org/10.1021/la0513858

Celik, Dominici, Filby, Das, Madden, & Paunov. (2019). Fabrication of Human Keratinocyte Cell Clusters for Skin Graft Applications by Templating Water-in-Water Pickering Emulsions. *Biomimetics*, *4*(3), 50. https://doi.org/10.3390/biomimetics4030050

Chen, Y., Wei, W., Zhu, Y., Luo, J., Liu, R., & Liu, X. (2020). Synthesis of Temperature/pH Dual-Stimuli-Response Multicompartmental Microcapsules via Pickering Emulsion for Preprogrammable Payload Release. *ACS Applied Materials and Interfaces*, *12*(4), 4821–4832. https://doi.org/10.1021/acsami.9b20999

Crepon, B., Jozefonvicz, J., Chytry, V., Rihova, B., & Kopecek, J. (1991). Enzymatic degradation and immunogenic properties of derivatized dextrans. *Biomaterials*, *12*(6), 550–554. https://doi.org/10.1016/0142-9612(91)90049-G

Destribats, M., Gineste, S., Laurichesse, E., Tanner, H., Leal-Calderon, F., Héroguez, V., & Schmitt, V. (2014). Pickering emulsions: What are the main parameters determining the emulsion type and interfacial properties? *Langmuir*, *30*(31), 9313–9326. https://doi.org/10.1021/la501299u

Dupont, H., Maingret, V., Schmitt, V., & Héroguez, V. (2021). New Insights into the Formulation and Polymerization of Pickering Emulsions Stabilized by Natural Organic Particles. *Macromolecules*, *54*(11), 4945–4970. https://doi.org/10.1021/acs.macromol.1c00225

El Founi, M., Soliman, S. M. A., Vanderesse, R., Acherar, S., Guedon, E., Chevalot, I., Babin, J., & Six, J. L. (2018). Light-sensitive dextran-covered PNBA nanoparticles as triggered

drug delivery systems: Formulation, characteristics and cytotoxicity. *Journal of Colloid and Interface Science*, *514*, 289–298. https://doi.org/10.1016/j.jcis.2017.12.036

Franssen, O., Van Ooijen, R. D., De Boer, D., Maes, R. A. A., & Hennink, W. E. (1999). Enzymatic degradation of cross-linked dextrans. *Macromolecules*, *32*(9), 2896–2902. https://doi.org/10.1021/ma981759m

Gautier, F., Destribats, M., Perrier-Cornet, R., Dechézelles, J.-F., Giermanska, J., Héroguez, V., Ravaine, S., Leal-Calderon, F., & Schmitt, V. (2007). Pickering emulsions with stimulable particles: from highly- to weakly-covered interfaces. *Physical Chemistry Chemical Physics*, *9*(48), 6455. https://doi.org/10.1039/b710226g

Glasing, J., Jessop, P. G., Champagne, P., & Cunningham, M. F. (2018). Graft-modified cellulose nanocrystals as CO2-switchable Pickering emulsifiers. *Polymer Chemistry*, *9*(28), 3864–3872. https://doi.org/10.1039/c8py00417j

Harman, C. L. G., Patel, M. A., Guldin, S., & Davies, G. L. (2019). Recent developments in Pickering emulsions for biomedical applications. *Current Opinion in Colloid and Interface Science*, *39*, 173–189. https://doi.org/10.1016/j.cocis.2019.01.017

Kaewprapan, Kulthida, Inprakhon, P., Marie, E., & Durand, A. (2012). Enzymatically degradable nanoparticles of dextran esters as potential drug delivery systems. *Carbohydrate Polymers*, *88*(3), 875–881. https://doi.org/10.1016/j.carbpol.2012.01.030

Kaewprapan, Kultida, Wongkongkatep, J., Panbangred, W., Phinyocheep, P., Marie, E., Durand, A., & Inprakhon, P. (2011). Lipase-catalyzed synthesis of hydrophobically modified dextrans: Activity and regioselectivity of lipase from Candida rugosa. *Journal of Bioscience and Bioengineering*, *112*(2), 124–129. https://doi.org/10.1016/j.jbiosc.2011.04.004

Kalashnikova, I., Bizot, H. H., Cathala, B., & Capron, I. (2011). New Pickering Emulsions Stabilized by Bacterial Cellulose Nanocrystals. *Langmuir*, *27*(12), 7471–7479.

https://doi.org/10.1021/la200971f

Lavis, L. D., & Raines, R. T. (2008). Bright ideas for chemical biology. *ACS Chemical Biology*, *3*(3), 142–155. https://doi.org/10.1021/cb700248m

Liechty, W. B., Kryscio, D. R., Slaughter, B. V., & Peppas, N. A. (2010). Polymers for drug delivery systems. *Annual Review of Chemical and Biomolecular Engineering*, *1*, 149–173. https://doi.org/10.1146/annurev-chembioeng-073009-100847

Liu, H., Wang, C., Zou, S., Wei, Z., & Tong, Z. (2012). Simple, reversible emulsion system switched by pH on the basis of chitosan without any hydrophobic modification. *Langmuir*, *28*(30), 11017–11024. https://doi.org/10.1021/la3021113

Maingret, V., Courrégelongue, C., Schmitt, V., & Héroguez, V. (2020). Dextran-Based Nanoparticles to Formulate pH-Responsive Pickering Emulsions: A Fully Degradable Vector at a Day Scale. *Biomacromolecules*, *21*(12), 5358–5368. https://doi.org/10.1021/acs.biomac.0c01489

Maingret, V., Schmitt, V., & Héroguez, V. (2021). Spatio-temporal control over destabilization of Pickering emulsions stabilized by light-sensitive dextran-based nanoparticles. *Carbohydrate Polymers*, *269*(April), 118261. https://doi.org/10.1016/j.carbpol.2021.118261

Nie, Z., Jai, I. P., Li, W., Bon, S. A. F., & Kumacheva, E. (2008). An "inside-out" microfluidic approach to monodisperse emulsions stabilized by solid particles. *Journal of the American Chemical Society*, *130*(49), 16508–16509. https://doi.org/10.1021/JA807764M/SUPPL_FILE/JA807764M_SI_001.PDF

Nouvel, C., Raynaud, J., Marie, E., Dellacherie, E., Six, J. L., & Durand, A. (2009). Biodegradable nanoparticles made from polylactide-grafted dextran copolymers. *Journal of Colloid and Interface Science*, *330*(2), 337–343. https://doi.org/10.1016/j.jcis.2008.10.069

Pang, S. C., Chin, S. F., Tay, S. H., & Tchong, F. M. (2011). Starch-maleate-polyvinyl alcohol hydrogels with controllable swelling behaviors. *Carbohydrate Polymers*, *84*(1), 424–429. https://doi.org/10.1016/j.carbpol.2010.12.002

Pickering, S. U. (1907). CXCVI.—Emulsions. *Journal of the Chemical Society, Transactions, 91*, 2001–2021. https://doi.org/10.1039/CT9079102001

Qi, L., Luo, Z., & Lu, X. (2018). Facile synthesis of starch-based nanoparticle stabilized Pickering emulsion: Its pH-responsive behavior and application for recyclable catalysis. *Green Chemistry*, *20*(7), 1538–1550. https://doi.org/10.1039/c8gc00143j

Ramsden, W. (1903). Separation of solids in the surface-layers of solutions and 'suspensions' (observations on surface-membranes, bubbles, emulsions, and mechanical coagulation).—Preliminary account. *Proc. Roy. Soc.*, *72*, 156–164.

Ren, W., Cai, R., Yan, W., Lyu, M., Fang, Y., & Wang, S. (2018). Purification and characterization of a biofilm-degradable dextranase from a marine bacterium. *Marine Drugs*, *16*(2), 1–16. https://doi.org/10.3390/md16020051

Ridel, L., Bolzinger, M. A., Gilon-Delepine, N., Dugas, P. Y., & Chevalier, Y. (2016). Pickering emulsions stabilized by charged nanoparticles. *Soft Matter*, *12*(36), 7564–7576. https://doi.org/10.1039/c6sm01465h

Rouzes, C., Leonard, M., Durand, A., & Dellacherie, E. (2003). Influence of polymeric surfactants on the properties of drug-loaded PLA nanospheres. *Colloids and Surfaces B: Biointerfaces*, *32*(2), 125–135. https://doi.org/10.1016/S0927-7765(03)00152-8

Sakellari, G. I., Zafeiri, I., Pawlik, A., Kurukji, D., Taylor, P., Norton, I. T., & Spyropoulos, F. (2021). Independent co-delivery of model actives with different degrees of hydrophilicity from oil-in-water and water-in-oil emulsions stabilised by solid lipid particles via a Pickering mechanism: a-proof-of-principle study. *Journal of Colloid and Interface Science*, *587*, 644–649. https://doi.org/10.1016/j.jcis.2020.11.021

Schmitt, V., Destribats, M., & Backov, R. (2014). Colloidal particles as liquid dispersion stabilizer: Pickering emulsions and materials thereof. *Comptes Rendus Physique*, *15*(8–9), 761–774. https://doi.org/10.1016/j.crhy.2014.09.010

Schröder, A., Laguerre, M., Sprakel, J., Schroën, K., & Berton-Carabin, C. C. (2020). Pickering particles as interfacial reservoirs of antioxidants. *Journal of Colloid and Interface Science*, *575*, 489–498. https://doi.org/10.1016/j.jcis.2020.04.069

Tang, J., Quinlan, P. J., & Tam, K. C. (2015). Stimuli-responsive Pickering emulsions: Recent advances and potential applications. *Soft Matter*, *11*(18), 3512–3529. https://doi.org/10.1039/c5sm00247h

Trofymchuk, K., Valanciunaite, J., Andreiuk, B., Reisch, A., Collot, M., & Klymchenko, A. S. (2019). BODIPY-loaded polymer nanoparticles: Chemical structure of cargo defines leakage from nanocarrier in living cells. *Journal of Materials Chemistry B*, *7*(34), 5199–5210. https://doi.org/10.1039/c8tb02781a

Vercauteren, R., Schacht, E., & Duncan, R. (1992). Effect of the Chemical Modification of Dextran on the Degradation by Rat Liver Lysosomal Enzymes. *Journal of Bioactive and Compatible Polymers*, *7*(4), 346–357. https://doi.org/10.1177/088391159200700404

Vignati, E., Piazza, R., & Lockhart, T. P. (2003). Pickering emulsions: Interfacial tension, colloidal layer morphology, and trapped-particle motion. *Langmuir*, *19*(17), 6650–6656. https://doi.org/10.1021/la034264l

Villemson, A., Couvreur, P., Gillet, B., Larionova, N., & Gref, R. (2006). Dextran-poly-ε-caprolactone micro- and nanoparticles: Preparation, characterization and tamoxifen solubilization. *Journal of Drug Delivery Science and Technology*, *16*(4), 307–313. https://doi.org/10.1016/S1773-2247(06)50055-3

Whitesides, T. H., & Ross, D. S. (1995). Experimental and Theoretical Analysis of the Limited Coalescence Process: Stepwise Limited Coalescence. *Journal of Colloid and*

Interface Science, *169*(1), 48–59. https://doi.org/10.1006/jcis.1995.1005

Ydens, I., Degée, P., Nouvel, C., Dellacherie, E., Six, J. L., & Dubois, P. (2005). "Surfactant-free" stable nanoparticles from biodegradable and amphiphilic poly(ε-caprolactone)-grafted dextran copolymers. *E-Polymers*, *046*, 1–11. https://doi.org/10.1515/epoly.2005.5.1.486